DESIGN AND THREE DIMENSIONAL MAGNET MAPPING AND CALCULATION FOR THE HERA CORRETION DIPOLES.

G.Woebke, H.Wuempelmann, U.Berghaus, W.-R.Novender
Deutsches Elektronen Synchrotron DESY, Notkestraße 85, 2000 Hamburg 52, W.Germany

Abstract: In order to correct the beam in the electron ring of the double storage ring HERA, two types of correction dipoles are required: Type CH, Type CV. Both types of dipoles have the same yoke and the same air cooled coils. They differ from each other in their pole plates only. By changing the pole plates, the pole distance can be easily varied.
The magnetic fields of the two magnet types are measured and compared with 3D field calculations done with the computer code PROFI [1]. The comparision shows very good agreement.

Design of the correction dipoles

Yoke

The complete yoke (figure 1.) for the correction dipoles consists of a laminated yoke with a length of 200 mm and the pole plates CH or CV with a length of 300 mm. The pole plates are joined to the yoke on each end by angle bars.

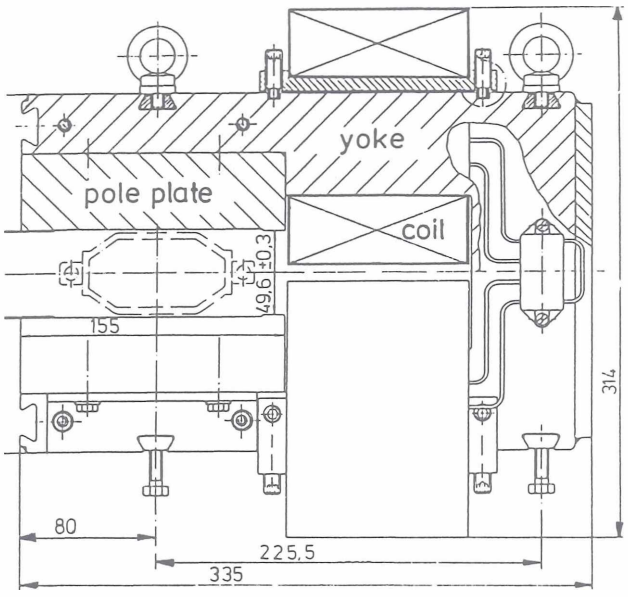

Fig. 1. correction dipole CH

The yokes are made of 5 mm-thick fine-blanked laminations and 1 mm- and 1.5 mm-thick compensating laminations stacked to the required length in a precision stacking fixture, and pressed and welded to the reinforcement plate at the rear of the yoke.
The pole plates consist of massive, hot-rolled, low-carbon steel. The CH-plate is 45.35 mm thick and 155 mm wide. The CV-plate is 25.1 mm thick and 170 mm wide. Both types of pole plates have two projecting ridges (CH: 19.7 mm x 0.75 mm and 13.2 mm x 0.95 mm; CV: 45 mm x 1.0 mm and 20 mm x 1.0 mm) to improve the horizontal field homogeneity.

Technical data

	Type CH	Type CV
Field strength at beam axis	:0.152 T	0.1075 T
Magnetic length	: 369 mm	387 mm
Cross-sectional area of coil	:3389 mm^2	3389 mm^2
Number of turns per coil	:1332	1332
Rated current	:2.4 A	3 A
Max. current density	:0.94 A/mm^2	1.18 A/mm^2
Power loss at rated current	:0.098 kW	0.153 kW

Coils

The correction dipole has 2 coils, each with 1332 turns of varnish-insulated copper wire conductor 1.8 mm in diameter. The turns are arranged in 24 layers, 12 of 55 turns each and 12 of 56 turns each. The coils are wound and vacuum impregnated in a u-shaped former. The side wall insulation (0.5 mm precut epoxy glass laminate) and the inner insulation (0.5 mm woven glass) are fixed in the former before winding starts. The outer insulation consists of 1 mm woven glass.

Magnet mapping

The magnetic fields of the two magnet types are measured with a high resolution temperature stabilized Hall probe assembled on a 1.5 m long laminated paper arm (figure 2.). The 3-D movement is made with an x,y,z-table driven by 2-phase step- by step motors.

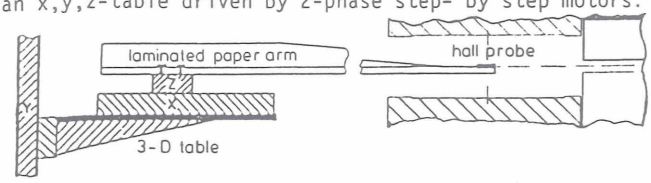

Fig. 2. measuring device

The CH and CV fields are measured along the beam axis. Two of the 460 measuring points within the range 0<z<470 mm are shown in figures 3. and 4. and compared with the 3-D field calculations. [2]

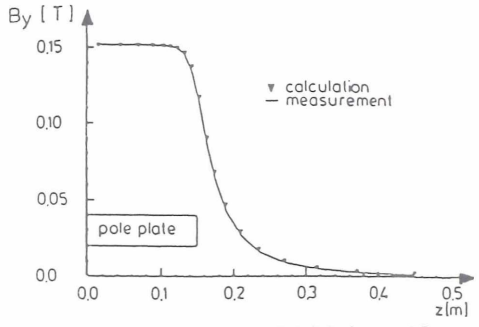

Fig. 3. correction dipole CH:B(z), x=35 mm, y=5 mm

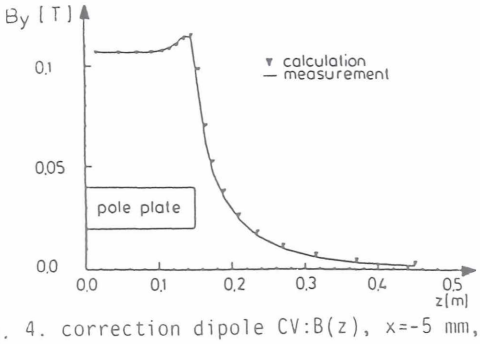

Fig. 4. correction dipole CV:B(z), x=-5 mm, y=35 mm

Field calculation

For reasons of symmetry it is only necessary to study a quarter of the magnet. The planes of symmetry are the xy- and xz-planes passing through the origin of the coordinates as in figure 5. The x-coordinate for the reference point (y=0,z=0) was taken from the first measurements. In the non symmetry planes,

the size of the region chosen for the calculation was 4 to 5 times greater than the external dimensions of the magnet. It is reasonably realistic to assume that the normal or tangential component of B at the boundary is equal to zero.
Only current filaments can be specified for the three-dimensional calculation. In order to take account of the spatial extent of the coil assembly, the 1332 turns were replaced by 4 current filaments distributed uniformly over the cross-section of the coil. Calculations with 40 conductor elements produced a reduction of less than 0.5 gauss in the air gap field, with a nominal field of approximately 1100 gauss. The more uniform current distribution made its effect felt in the direction of the coil: at a distance of 30 mm or more from the beam axis the influence became more clearly recognizable, and at 60 mm it produced a deviation of approximately 7 gauss. A three-dimensional representation of the vertical correction magnet CV is given in figure 5.

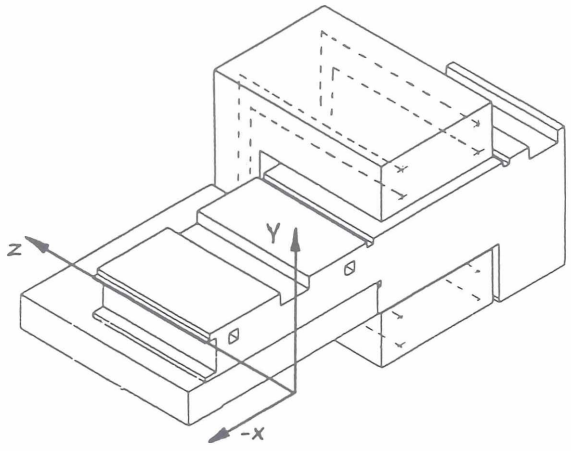

Fig. 5: 3-D view of a quarter magnet (dashed lines are curret filaments) and coordinate system

The 3-D grid needed for discretization comprised 26320 grid points, of which 9600 were accounted for by the complete magnet and 5040 by the section of the beam tube along the beam axis. For each grid point the program supplies the magnetic scalar potential and the three components of the induction B. The computing time for the iteration was about 35 - 40 CPU minutes IBM 3084 Q with a region size of 2 Mbytes. The calculation of the field was so exact that the mean variation in permeability of all the points in the iron from one iteration cycle to another came to < 0.2%.

Comparison between measurement and calculation

Out of the extensive measurements and calculations performed, the following are discussed in more detail (coordinates in mm):
Measurement 4: Type CH, $B=B_y(z)$, x=35, y=5

Measurement 13: Type CV, $B=B_y(z)$, x=-5, y=35

If the first measured value differed from the last measured value at the reference point, it would be possible to apply a linear correction to all the measured values, since the measurements were taken at constant intervals of time and the magnet was measured in the warmed-up state.
The results of the measurements and calculations along the beam axis were used to assess the field quality, the integral $\int B_y dz$ being evaluated for various integration paths along the z-axis. The tables 1 and 2 provide a comparison of the two results in absolute figures for both types of magnet:

z-axis		$\int$ Bdz [Tm]		diff.
x	y	measured	calculated	%
-35	5	0.0277861	0.0287271	3.38
-25	5	0.0278416	0.0287710	3.33
-15	5	0.0278758	0.0287988	3.31
-5	5	0.0278916	0.0288192	3.32
5	5	0.0278892	0.0288146	3.31
15	5	0.0278718	0.0287959	3.31
25	5	0.0278305	0.0287644	3.35
35	5	0.0277659	0.0287109	3.40
-35	15	0.0278387	0.0287334	3.21
-25	15	0.0278913	0.0287812	3.19
-15	15	0.0279247	0.0288102	3.17
-5	15	0.0279340	0.0288310	3.21
5	15	0.0279339	0.0288270	3.19
15	15	0.0279214	0.0288094	3.18
25	15	0.0278892	0.0287795	3.19
35	15	0.0278345	0.0287306	3.21

Table 1: Type CH (Measurement 4)

z-axis		$\int$ Bdz [Tm]		diff.
x	y	measured	calculated	%
-25	5	0.0207876	0.0218867	5.28
-15	5	0.0208238	0.0218733	5.03
-5	5	0.0208399	0.0218459	4.82
5	5	0.0208393	0.0218172	4.69
15	5	0.0208235	0.0217807	4.59
25	5	0.0207917	0.0217336	4.53
-25	15	0.0208400	0.0218891	5.03
-15	15	0.0208572	0.0218756	4.88
-5	15	0.0208695	0.0218521	4.70
5	15	0.0208703	0.0218264	4.58
15	15	0.0208574	0.0217931	4.48
25	15	0.0208294	0.0217511	4.42

Table 2: Type CV (Measurement 13)

While the integral field shows variations in the order of percents between the absolute figures for the measured and calculated values, the relative field qualities (relative lens aberration) compare very well. The deviation in the absolute figures is due in general to the idealization of the magnetic field calculation, and also depends on:
- the constancy of the μ-curves (magnetic values) throughout the iron. In fact there are variations in the mean values of the batches supplied and in the individual measurements at different points on a given sheet of soft iron;
- the production accuracy of the lamination stamping, and the stacking accuracy of the yoke assemblies;
- the dimensional accuracy and internal distribution of the conductors in the field coils, especially with large numbers of turns (the calculation uses only four current filaments);
- the impairment of the magnetic properties of the assembled magnet as a result of stamping ridges, drilled and threaded holes, fixing bolts, and supports for coils and fittings.

Comparing measurements 4 and 13, we see an increase in the deviation from ~3% to ~5% as the pole gap widens from 51.5 mm to 92 mm, i.e., given the same grid, the greater the air gap for pole assemblies of identical length, the greater is the discrepancy between the measured and calculated values.
The variations in this deviation for various integration paths (particle trajectories) are considerably smaller, however. For measurement 4 the deviation lies between 3.17% and 3.40%, and for measurement 13 between 4.42% and 5.28%, so that a good measure of agreement can be expected when assessing relative field

qualities.
First we have to obtain the field integral in the unmeasured and uncalculated ideal path (beam axis) for calculation and measurement. This is derived by averaging from the adjacent trajectories $B_y(z)$ for x=-5 mm, y=5 mm and x=5 mm, y=5 mm on the assumption that the symmetrical configuration gives identical values for x=-5 mm, y=-5 mm and x=5 mm, y=-5 mm. The Table 3 shows the reference values $\int B_y(z)dz$ obtained by this means for x=0, y=0:

	measurement	calculation
Measurement 4 CH	0.02789045 Tm	0.0288169 Tm
Measurement 13 CV	0.02083965 Tm	0.02183155 Tm

Table 3: Measured/calculated values for measurement 4 and 13

The relative field quality of the magnets is obtained separately for the measured and calculated values, using the formula:

$$\Delta B_y = (\int B_y dz - \int B_y(0,0,z)dz) \; / \; \int B_y(0,0,z)dz$$

The results of this calculation are shown in the tables 4 and 5.

z-axis		relative field errors ΔB_y x 0.001		
x	y	measured	calculated	diff.
-35	5	-3.74	-3.12	0.62
-25	5	-1.75	-1.59	0.16
-15	5	-0.52	-0.63	0.11
-5	5	+0.04	+0.08	0.04
5	5	-0.04	-0.08	0.04
15	5	-0.67	-0.73	0.06
25	5	-2.15	-1.82	0.33
35	5	-4.47	-3.68	0.79
-35	15	-1.86	-2.90	1.04
-25	15	+0.03	-1.24	1.27
-15	15	+1.23	-0.23	1.46
-5	15	+1.56	+0.49	1.07
5	15	+1.56	+0.35	1.21
15	15	+1.11	-0.26	1.37
25	15	-0.04	-1.30	1.26
35	15	-2.00	-2.99	0.99

Table 4: Type CH (Measurement 4)

z-axis		relative field errors ΔB_y x 0.001		
x	y	measured	calculated	diff.
-25	5	-2.50	+2.53	5.03
-15	5	-0.76	+1.91	2.67
-5	5	+0.01	+0.66	0.65
5	5	-0.01	-0.66	0.65
15	5	-0.77	-2.33	1.56
25	5	-2.30	-4.49	2.19
-25	15	+0.02	+2.64	2.62
-15	15	+0.84	+2.02	1.18
-5	15	+1.43	+0.94	0.49
5	15	+1.47	-0.24	1.71
15	15	+0.85	-1.76	2.61
25	15	-0.49	-3.69	3.20

Table 5: Type CV (Measurement 13)

As can be seen from figure 6., the relative errors produced by the computer program PROFI are not only very close ($\leq 10^{-3}$) to the measurements, but also reproduce the shape well (ratio of air gap to pole length = 0.17).

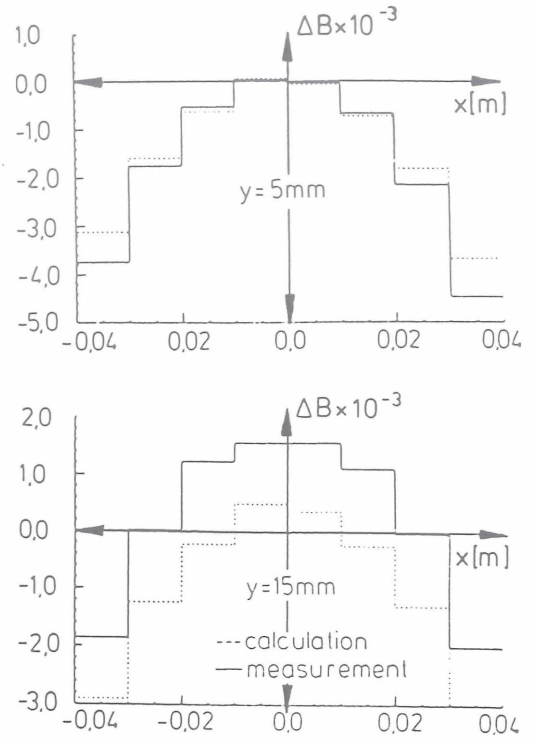

Figure 6.: relative field error CH

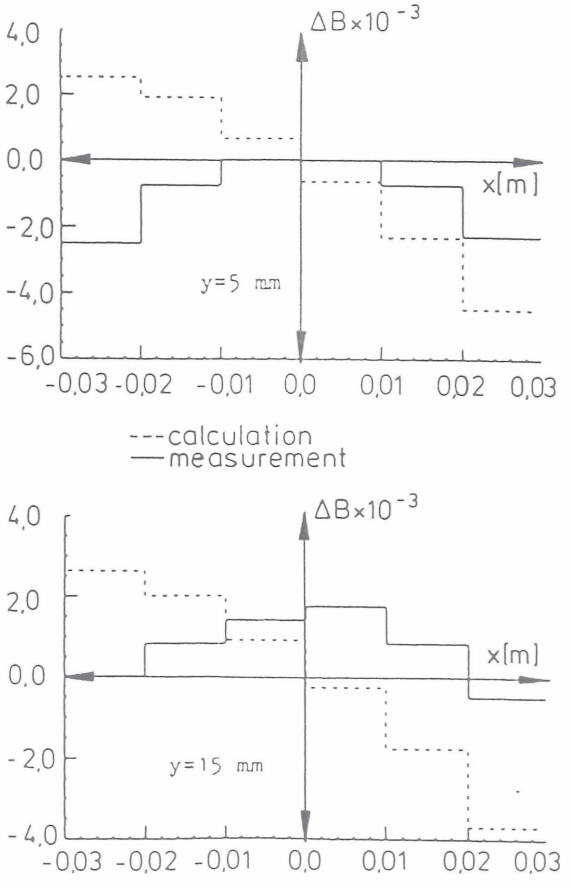

Figure 7.: relative field error CV

Figure 7. shows a markedly poorer reproduction of the measured values, but it is still $\leq 8 \times 10^{-3}$. The shape of the field distribution, which provides information on the presence of higher multipoles, is no longer reproduced, but it can be seen that it is the calculation that tends to yield the larger error (i.e. the magnet is better than previously calculated). While the measurement yields mainly sextupole components, the calculation produces mainly quadrupole components (ratio of air gap to pole length = 0.3).

Conclusions

The comparison of the absolute values obtained by measurement and calculation reveals that the results in the air gap are practically identical, while the calculated field is generally about 5% too high at the edge of the pole and approximately 1 - 2% too high towards the margins of the pole. This latter field deviation stems from the choice of boundary condition (normal component = 0). The error at the pole edges is due to a coarse grid density.
The evaluation of the field integrals yields, for an air gap/pole length ratio of 0.17, an absolute deviation of $\sim 3\%$ and a very good quantitative and qualitative reproduction of the field homogeneity ($\sim 1 \times 10^{-3}$). If the ratio is increased to 0.3 the absolute deviation is in the region of $\sim 5\%$, and that of the field error is $\sim 8 \times 10^{-3}$. The field shape is no longer correctly reproduced.
Given suitably careful choice of input values and grid for the program PROFI, good forecasts can be obtained even for small magnets with a large proportion of fringe fields.

References

[1] W. Müller et al: Numerical Solution of 2- or 3-Dimensional Nonlinear Field Problems by Means of the Computer Program PROFI, Archiv für Elektrotechnik 65 (1982)

[2] U.Berghaus, W.-R.Novender, Three Dimensional Magnet Mapping and Calculations for the Prototyp of the HERA Correction Dipoles. DESY M-86-09, October 1986